Excitation of Various Levels of C^{12} and O^{16} by 156-MeV Protons*

H. K. Lee
Duquesne University, Pittsburgh, Pennsylvania
AND
H. McManus
Michigan State University, East Lansing, Michigan
(Received 20 April 1967)

The cross sections and polarizations for the final states 1^-, 1^+, 2^-, 2^+, and 3^- of C^{12} and 1^-, 2^-, and 3^- of O^{16} are calculated using the Gillet vectors and the WKB method with the impulse approximation. The WKB method is found to work very well compared with the distorted-wave impulse approximation. Surprisingly good agreement is reached with cross-section data for most cases. Agreement with polarization data is poor. There exists a striking correlation between inelastic electron and proton scattering.

I. INTRODUCTION

THE purpose of the present investigation is to study the inelastic scattering of 156-MeV protons by the target nuclei C^{12} and O^{16}. The scattering matrix for nuclear reactions involves two distinct terms, the distorted waves of the projectile and the nuclear form factors. To compute the distorted waves, we use the WKB method. In order to check the validity of the WKB method, we compare, whenever possible, present calculations with the work of Haybron and McManus,[1,2] who treated the distorted waves "exactly". Unlike the potentials used in most WKB calculations,[3] the optical potentials used here are more realistic and contain spin-orbit terms as first treated by Hooton and Ashcroft.[4] The effect of the optical potentials on the polarization is studied. To simplify the calculation of the form factors, we use a version of the impulse approximation which essentially allows the use of free two-nucleon scattering amplitudes in place of the two-nucleon pseudopotential. Then the form factors may be calculated from the nuclear wave functions as determined by Gillet and Vinh-Mau[5] on the basis of the particle-hole model. As there are no free parameters appearing in the scattering amplitude, we are able to test the accuracy of the nuclear wave functions and thus the particle-hole model. Calculations are performed for the theoretical levels 1^- $T=1$ (21.5 MeV), 1^+ $T=0$ (14 MeV), 1^+ $T=1$ (16.6 MeV), 2^- $T=0$ (15.6, 16, and 21.2 MeV), 2^- $T=1$ (19.3 and 23.2 MeV), 2^+ $T=0$ (4.8 MeV), 2^+ $T=1$ (16.3 MeV), 3^- $T=0$ (12.8 and 19.5 MeV), and 3^- $T=1$ (23.5 MeV), of C^{12}; and for the levels 1^- $T=1$ (13.5 MeV), 2^- $T=0$ (10.5, 14.6, 16.6, and 17.3 MeV), 2^- $T=1$ (13, 17.6, 19.1, and 20.2 MeV), 3^- $T=0$ (6.15, 15.1, and 20.1 MeV), of O^{16}. Attempts are made to identify the levels observed in high-energy inelastic proton-scattering experiments (Fig. 1).

In Sec. II, we define various terms that appear in the scattering amplitude. Reduction of the scattering amplitude and detailed calculations of the relevant quantities are outlined in Sec. III. The results of the present investigation are discussed in comparison with experimental data in Sec. IV. Conclusions are drawn in Sec. V.

II. SCATTERING AMPLITUDE

In the distorted-wave impulse approximation (DWIA),[6-8] the scattering amplitude of inelastically scattered nucleons from closed-shell nuclei is given in the center-of-mass system:

$$S(J_f,M_f,T_f)=2\left(\frac{k}{k_0}\right)^{1/2}\left(\frac{N}{1+N}\right)\sum_{\substack{S,m\\L,M}}(-1)^m \times\langle L,S,M,m\,|\,J_f,M_f\rangle\int\chi_{\mathbf{k}}^{(-)*}M_{S,T_f}{}^m Y_L{}^{M*}(\theta,\phi) \times F^{L\,S\,J_f,T_f}(r)\chi_{\mathbf{k}_0}^{(+)}d^3r, \quad (1)$$

where

$$F^{L\,S\,J_f,T_f}(r)=\sum_{\alpha,\beta}\sqrt{2}\frac{\hat{j}_\alpha}{\hat{J}_f}(X+Y)_{\alpha,\beta}(-1)^{j_\beta+1/2} \times\langle(l_\alpha,s_\alpha)j_\alpha\|T_{LS,J_f}\|j_\beta(l_\beta,s_\beta)\rangle \times R_{n\alpha,l\alpha}{}^*(r)R_{n\beta,l\beta}(r). \quad (2)$$

The scattering matrix describes the transition of target nuclei from the ground state ($J_0=T_0=0$) to an excited particle-hole state with total angular momentum J_f, projection M_f, and isospin T_f. $\chi_{\mathbf{k}_0}^{(+)}$ and $\chi_{\mathbf{k}}^{(-)*}$ are the distorted waves of the projectile with wave numbers $\mathbf{k}_0$ and $\mathbf{k}$ before and after the collision. Equation (2)

* Research supported in part by the U. S. Atomic Energy Commission.

[1] R. Haybron and H. McManus, Phys. Rev. **136**, B1730 (1964).
[2] R. Haybron and H. McManus, Phys. Rev. **140**, B638 (1965).
[3] E. J. Squires, Nucl. Phys. **6**, 504 (1958); E. A. Sanderson, *ibid.* **35**, 557 (1962); D. Jackson, *ibid.* **35**, 194 (1962).
[4] D. J. Hooton and N. Ashcroft, Proc. Phys. Soc. (London) **81**, 193 (1963).
[5] V. Gillet and N. Vinh-Mau, Nucl. Phys. **54**, 321 (1964).
[6] A. Kerman, H. McManus and R. Thaler, Ann. Phys. (N. Y.) **8**, 551 (1959).
[7] T. Erickson, Nucl. Phys. **54**, 321 (1964).
[8] H. K. Lee, thesis, Michigan State University, 1966 (unpublished).

defines the nuclear form factors. n_α, l_α, s_α, and j_α are the principal quantum number, the orbital angular momentum, the spin, and the total angular momentum of the particle, respectively; n_β, l_β, s_β, and j_β have similar meanings for the hole. $(X+Y)$ are the relative strengths of a given particle-hole pair as listed in Ref. 5. $\sqrt{2}$ in (2) is the result of taking matrix elements of the isospin operators. $\hat{J}_f=(2J_f+1)^{1/2}$, etc. $\langle\|\, T\,\|\rangle$ is the reduced matrix element[9] of the operator

$$T_{LS,J\mu}=\sum_{M',m'}\langle L,S,M',m'\,|\,J,\mu\rangle Y_L{}^{M'}(\theta_i,\phi_i)\sigma_S{}^{m'}(i)\,,$$

where i refers to a nucleon in the target.

$M_{S,T_f}{}^m$ is an operator in the spin space of the projectile. If we take the unit vectors $\hat{p}$, $\hat{q}$, $\hat{n}$ as defined by Kerman, McManus, and Thaler (KMT) (Ref. 6), and choose the z direction to coincide with $\hat{p}$, we have

$$\begin{aligned}
&M_{0,T_f}{}^0=A+C\boldsymbol{\sigma}\cdot\hat{n}\,,\\
&M_{1,T_f}{}^0=F\boldsymbol{\sigma}\cdot\hat{p}\,,\\
&M_{1,T_f}{}^1=-(i/\sqrt{2})[B\boldsymbol{\sigma}\cdot\hat{n}+C+iE\boldsymbol{\sigma}\cdot\hat{q}]\,,\\
&M_{1,T_f}{}^{-1}=-(i/\sqrt{2})[B\boldsymbol{\sigma}\cdot\hat{n}+C-iE\boldsymbol{\sigma}\cdot\hat{q}]\,.
\end{aligned}\tag{3}$$

In (3), A, B, C, E, and F are the various spin-isospin-dependent parts of the two-nucleon scattering amplitude. Their values are listed in Ref. 6 and these are the values used here for the two-nucleon interaction.

III. OUTLINE OF CALCULATIONS

A. Form Factors

Since the parity of the final nuclear state is a good quantum number, L in (1) can only be $L=J_f$ for the normal parity state and $L=J_f\pm1$ for the abnormal parity state. The reduced matrix element in (2) can be evaluated by using the relations of Brink and Satchler.[9]

$$F^{J_f,\,0,J_f,T_f}=\frac{\sqrt{2}}{(4\pi)^{1/2}}\sum_{\alpha,\beta}(X+Y)_{\alpha,\beta}(-1)^{2j_\beta+J_f}\hat{j}_\alpha\hat{j}_\beta\times\begin{pmatrix}j_\alpha & j_\beta & J_f\\ \frac{1}{2} & -\frac{1}{2} & 0\end{pmatrix}R_{n\alpha,l\alpha}{}^*(r)R_{n\beta,l\beta}(r)\,,\tag{4}$$

$$F^{J_f,\,1,J_f,T_f}=\frac{\sqrt{2}}{(4\pi)^{1/2}}\sum_{\alpha,\beta}(X+Y)_{\alpha,\beta}(-1)^{l_\alpha+j_\beta+1/2}\hat{j}_\alpha\hat{j}_\beta\times\begin{pmatrix}j_\alpha & j_\beta & J_f\\ \frac{1}{2} & \frac{1}{2} & -1\end{pmatrix}R_{n\alpha,l\alpha}{}^*(r)R_{n\beta,l\beta}(r)\tag{5}$$

for the normal parity states, and

$$F^{J_f-1,1,J_f,T_f}=\frac{\sqrt{2}}{(4\pi)^{1/2}}\sum_{\alpha,\beta}(X+Y)_{\alpha,\beta}\hat{L}\hat{j}_\alpha\hat{j}_\beta(-1)^{2j_\beta+l_\beta+l_\alpha+1}\begin{pmatrix}j_\alpha & j_\beta & J_f\\ \frac{1}{2} & -\frac{1}{2} & 0\end{pmatrix}\times\frac{[(l_\alpha-j_\alpha)(2j_\alpha+1)+(l_\beta-j_\beta)(2j_\beta+1)-J_f]}{[J_f(2J_f+1)(2J_f-1)]^{1/2}}R_{n\alpha,l\alpha}{}^*(r)R_{n\beta,l\beta}(r)\,,\tag{6}$$

$$F^{J_f+1,1,J_f,T_f}=\frac{\sqrt{2}}{(4\pi)^{1/2}}\sum_{\alpha,\beta}(X+Y)_{\alpha,\beta}\hat{L}\hat{j}_\alpha\hat{j}_\beta(-1)^{2j_\beta+l_\beta+l_\alpha+1}\begin{pmatrix}j_\alpha & j_\beta & J_f\\ \frac{1}{2} & -\frac{1}{2} & 0\end{pmatrix}\times\frac{[(l_\alpha-j_\alpha)(2j_\alpha+1)+(l_\beta-j_\beta)(2j_\beta+1)+J_f+1]}{[(J_f+1)(2J_f+1)(2J_f+3)]^{1/2}}R_{n\alpha,l\alpha}{}^*(r)R_{n\beta,l\beta}(r)\tag{7}$$

for the abnormal parity states. $R_{n,l}$ are assumed to be harmonic-oscillator eigenfunctions.[10] The harmonic-oscillator constants are $\alpha=m\omega/\hbar=0.37$ F^{-2} for C^{12} and $\alpha=0.311$ F^{-2} for O^{16}.[11] The form factors (4), (5), (6), and (7) have been evaluated and are listed in the Appendix.

B. Distorted Waves

In the WKB approximation[4,12] we have

$$\chi_{\mathbf{k}_0}{}^{(+)}=\frac{1}{(2\pi)^{3/2}}\exp\left(i\mathbf{k}_0\cdot\mathbf{r}-\frac{ik_0}{2E_0}\times\int_{-\infty}^{z}[W_1(b,z')+W_2(b,z')\boldsymbol{\sigma}\cdot\mathbf{b}\times\mathbf{k}_0]dz'\right),\tag{8}$$

[9] D. Brink and G. Satchler, *Angular Momentum* (Oxford University Press, London, 1962), Chap. 5, Appendices.

[10] M. G. Mayer and J. Jensen, *Elementary Theory of Nuclear Shell Model* (John Wiley & Sons, Inc., New York, 1955).

[11] L. Elton, *Nuclear Sizes* (Oxford University Press, London, 1961).

[12] G. P. McCauley and G. Brown, Proc. Phys. Soc. (London) **71**, 893 (1958).

$$\chi_k^{(-)*}=\frac{1}{(2\pi)^{3/2}}\exp\left(-i\mathbf{k}\cdot\mathbf{r}-\frac{ik}{2E}\times\int_z^\infty[W_1(b,z')+W_2(b,z')\boldsymbol{\sigma}\cdot\mathbf{b}\times\mathbf{k}]dz'\right). \quad (9)$$

W_1 and W_2 are the central and spin-orbit parts of the optical potential. Functional forms and parameters for W_1 and W_2 for C^{12} have been determined from elastic proton scattering.[13] The parameters of the optical potential for O^{16} are assumed to be the same as those for C^{12}. b is the impact parameter defined by $\mathbf{r}=(x,y,z)=(\mathbf{b},z)$. We make the small-angle approximation and assume that the energy loss by the projectile is small compared to the incoming energy. For later use, we define the following quantities:

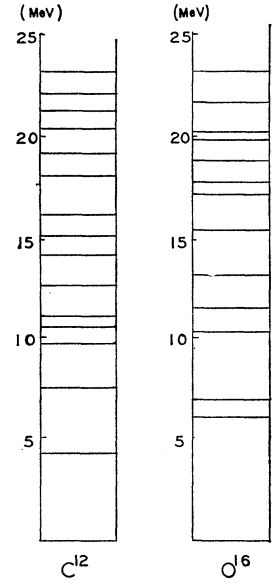

FIG. 1. Levels observed in high-energy inelastic-proton-scattering experiments at Uppsala and Orsay. (See Refs. 16, 20, and 23.)

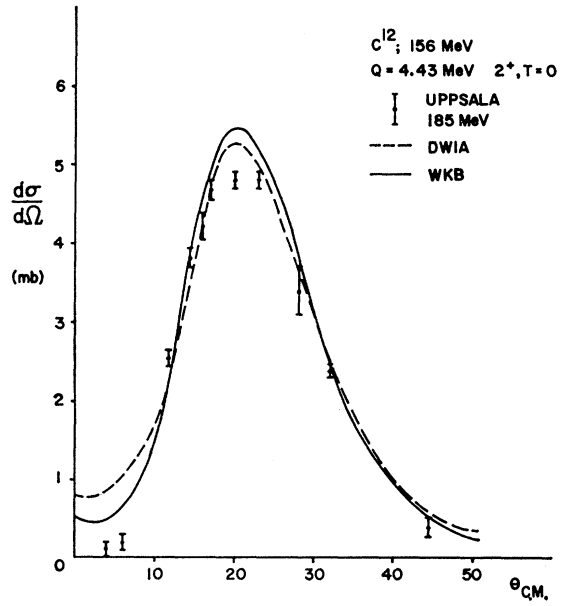

FIG. 2. The 2^+ $T=0$ level at 4.43 MeV of C^{12}. The WKB curve is in good agreement with DWIA result (Ref. 2) and data (Ref. 16).

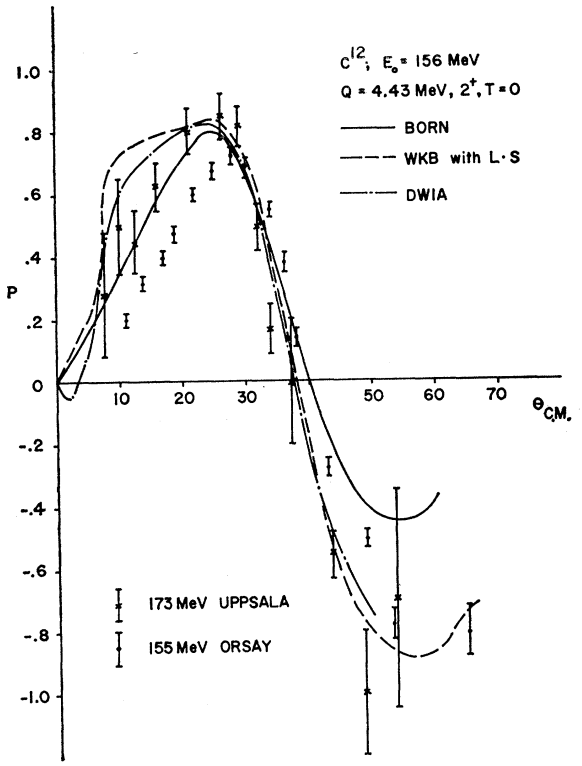

FIG. 3. Polarization due to excitation of 2^+ $T=0$ level at 4.43 MeV of C^{12}. Agreement between theoretical curves and Uppsala data (Ref. 19) is reasonable, but compared with more recent data from Orsay (Ref. 18), the spin-orbit terms in the optical potential affect the Born approximation in the wrong way at small angles. Agreement between WKB and DWIA is good.

$$\Gamma(b)=\exp\left(-\frac{ik_0}{2E_0}\int_{-\infty}^{+\infty}W_1(b,z')dz'\right), \quad (10)$$

$$Q_1(b)=\frac{bk_0^2}{2E_0}\int_{-\infty}^{z}W_2(b,z')dz', \quad (11)$$

$$Q_2(b)=\frac{bk_0^2}{2E_0}\int_{z}^{\infty}W_2(b,z')dz', \quad (12)$$

$$Q=Q_1+Q_2,\quad Q'=Q_1-Q_2. \quad (13)$$

$\Gamma(b)$ and $Q(b)$ are evaluated numerically and the results are fitted to suitable functions as shown in the following:

$$\Gamma(b)=1-e^{-Ab^2}(V_1+V_2b^2)-e^{-Bb^2}(V_3+V_4b^2), \quad (14)$$

$$Q(b)=-\frac{k_0^2}{E_0}\left(\frac{\hbar}{m_\pi c}\right)^2(V_s+iW_s)\times[(Y_1b+Y_2b^3)e^{-Rb^2}+(Y_3b+Y_4b^3)e^{-Sb^2}], \quad (15)$$

[13] G. Satchler and R. Haybron, Phys. Letters 11, 313 (1964).

TABLE I. Fittings of the distorted waves. $\Gamma(b)=1-e^{-Ab^2}(V_1+V_2b^2)-e^{-Bb^2}(V_3+V_4b^2)$; $Q(b)=-(k_0^2/E_0)(\hbar/m_\pi c)^2 \times(V_s+iW_s)[e^{-Rb^2}(Y_1b+Y_2b^3)+e^{-Sb^2}(Y_3b+Y_4b^3)]$.

	V_1	V_2	V_3	V_4	A	B	Y_1	Y_2	Y_3	Y_4	R	S
C^{12}	1.613	−0.046	−1.078	−0.127	0.17	0.39	0.783	−0.101	−0.315	0.520	0.3	0.39
O^{16}	3.154	−0.035	−2.586	−0.269	0.2	0.35	−348.7	−11.58	349.2	−5.64	0.5	0.45

where $(\hbar/m_\pi c)$ is the π-meson Compton wavelength and V_s and W_s are given in Ref. 13. The constants A, B, V_1, $\cdots$, V_4 and R, S, Y_1, $\cdots$, Y_4 are listed in Table I.

C. Evaluation of the Scattering Amplitude

To reduce the scattering amplitude further, we make the following approximations[4]:

$$e^{-iQ_2\sigma_\mu\sigma_\nu}e^{-iQ_1\sigma_\mu}=\sigma_\nu-i\sigma_\nu\sigma_\mu Q+\tfrac{1}{2}i(Q-Q')[\sigma_\nu,\sigma_\mu] \quad (16)$$

$$=\sigma_\nu-i\sigma_\nu\sigma_\mu Q+\tfrac{1}{2}iQ[\sigma_\nu,\sigma_\mu]. \quad (17)$$

The relation (16) is the result of assuming Q_1 and Q_2 to be small. In Eq. (17), we ignore $Q'(b,z)$. This is done for computational convenience. Cross sections are affected very little by $Q'(b,z)$. We have calculated the polarizations due to the transitions to 2^+, 2^-, and 1^+ states of C^{12} with and without $Q'(b,z)$. The differences are found to be small. Thus we use Eq. (17) throughout this work.

With Eqs. (14), (15), and (17), we can expand the scattering amplitude in the Pauli spin operators of the projectile.

$$S=S^0\mathbf{1}+S^x\sigma_x+S^y\sigma_y+S^z\sigma_z. \quad (18)$$

Cross sections and polarizations can be computed using the usual formulas (Ref. 7). The coefficients S^0, S^x, S^y, and S^z involve integrals of the type

$$I=\int e^{-iq\cdot r}\Gamma(b)Q(b)F^{LSJ_f,T_f}(r)Y_L{}^{M*}(\theta,\phi)d^3r. \quad (19)$$

Integration can be done analytically by using the formula[14,15]

$$\frac{1}{2\pi i^m}\int_0^{2\pi}e^{iz\cos\phi}\cos m\phi\, d\phi=J_m(z), \quad (20)$$

$$\int_0^\infty e^{-\alpha b^2}J_\nu(qb)b^{\mu-1}db=\frac{\Gamma(\frac{1}{2}\nu+\frac{1}{2}\mu)(q/2\sqrt{\alpha})^\nu}{2\alpha^{\mu/2}\Gamma(1+\nu)} \times e^{-q^2/4\alpha}\,{}_1F_1(\tfrac{1}{2}\nu-\tfrac{1}{2}\mu+1;1+\nu;q^2/4\alpha), \quad (21)$$

where J_ν is the Bessel function,

$${}_1F_1(\lambda,\rho,z)=\sum_{n=0}^{\infty}\frac{(\lambda)_n z^n}{n!(\rho)_n},$$

$$(\lambda)_0=1,\quad (\lambda)_n=\lambda(1+\lambda)\cdots(\lambda+n-1),$$

and

$$\Gamma(n)=(n-1)!.$$

For our calculation the F's turn out to be polynomials of finite degree. It may also be shown with the aid of (20) that (19) is zero unless $L+M=$ even.

IV. RESULTS AND DISCUSSION

A. C^{12}

1. $Q=4.43$ MeV: 2^+ $T=0$.

The differential cross sections predicted by WKB and DWIA (Ref. 2) and the experimental data[16] are plotted in Fig. 2. (See also Fig. 1.) The two calculations differ by only a few percent over most of the range of momentum transfer. Agreement with experiment is good, supporting the conclusion reached by analysis of electron scattering [17] that the theoretical form factor given by the particle-hole model in the random-phase approximation is, rather surprisingly, adequate over a fair range of momentum transfer.

The polarization predicted is compared with data[18,19]

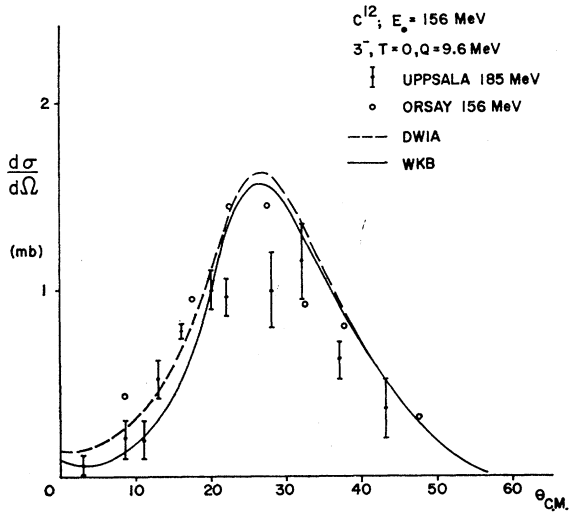

FIG. 4. Differential cross section for the 3^- $T=0$ level at 9.6 MeV of C^{12}. Circles are from Ref. 20 and points with bars are due to Uppsala group (Ref. 16).

[14] P. Morse and H. Feshbach, *Methods of Theoretical Physics* (McGraw-Hill Book Company, Inc., New York, 1953), Vol. II.
[15] G. Watson, *Theory of Bessel Functions* (The MacMillan Company, New York, 1945), 2nd ed.
[16] D. Hasselgren, P. Roenberg, O. Sunberg, and G. Tibell, Nucl. Phys. **69**, 81 (1965).
[17] V. Gillet and M. Melkanoff, Phys. Rev. **133**, B1190 (1964).
[18] N. Marty (private communications).
[19] P. Hillman, A. Johansson, and H. Tyren, Nucl. Phys. **4**, 648 (1957).

in Fig. 3. The spin-orbit optical term improves the agreement between theory and experiment considerably at larger angles 30°–70°. However, at small angles, the corrections induced by the optical spin-orbit are in the wrong direction, moving the predictions further away from experiment. This discrepancy persists if the magnitude of V_s (real part of the optical spin-orbit) is altered. Changing W_s (imaginary part of optical spin-orbit) has practically no effect. There is reasonably good agreement between the DWIA and WKB calculations of the polarization.

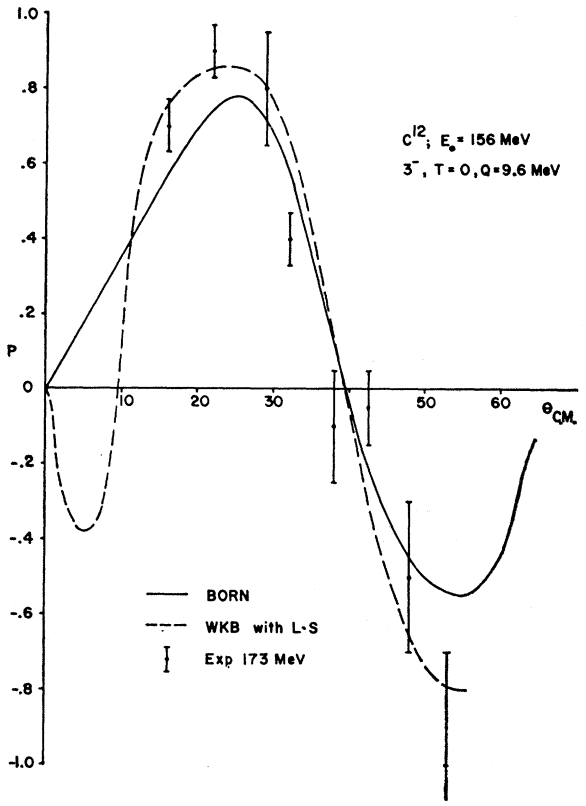

FIG. 5. Polarization due to the 3^- $T=0$ level at 9.6 MeV of C^{12}. DWIA curve of Ref. 2 is not shown as it is almost identical with WKB result. Data from Ref. 19.

2. $Q=9.6$ MeV: 3^- $T=0$

The form factor of this level is computed from the Gillet vector for the lowest 3^- $T=0$ state computed to lie at 12.8-MeV excitation. WKB and DWIA agree closely for both cross section and polarization. The predicted cross section (Fig. 4) agrees well with the Orsay data[20]; its shape, but not magnitude, agrees with measurements at Uppsala. The predicted polarization

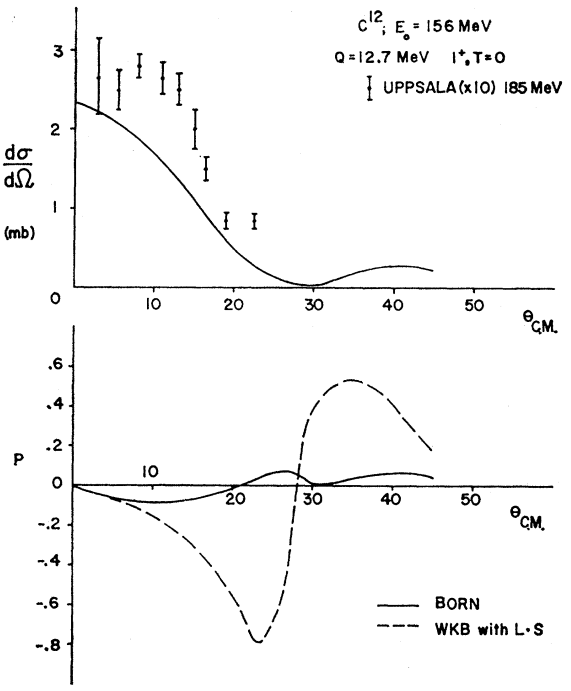

FIG. 6. Cross section and polarization of the 1^+ $T=0$ level at 12.7 MeV of C^{12}. Cross-section data (Ref. 16) are multiplied by 10. The effect of the spin-orbit term is large for the polarization. No DWIA calculation is available for comparison with WKB.

(Fig. 5) agrees well with experiment. In this case there is no small-angle polarization data. Again, the form factor used here gives fair agreement with electron scattering (Ref. 17) as far as peak magnitude and general shape are concerned.

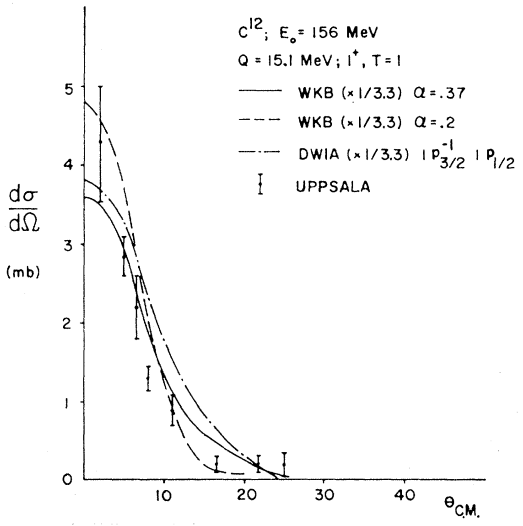

FIG. 7. Cross section of the 1^+ $T=1$ level at 15.1 MeV of C^{12}. All the theoretical curves have been reduced by a factor of 3.3 (see text). The form factor for DWIA calculation was computed with $(1p_{3/2})^{-1}\,1p_{1/2}$ configuration. α's are harmonic-oscillator constants. Data from Ref. 16.

[20] J. Jacmart, J. Garron, R. Riou, and C. Ruhla, *Direct Interactions and Nuclear Reaction Mechanism*, edited by E. Clemental and C. Villi (Gordon and Breach Science Publishers, Inc., New York, 1962).

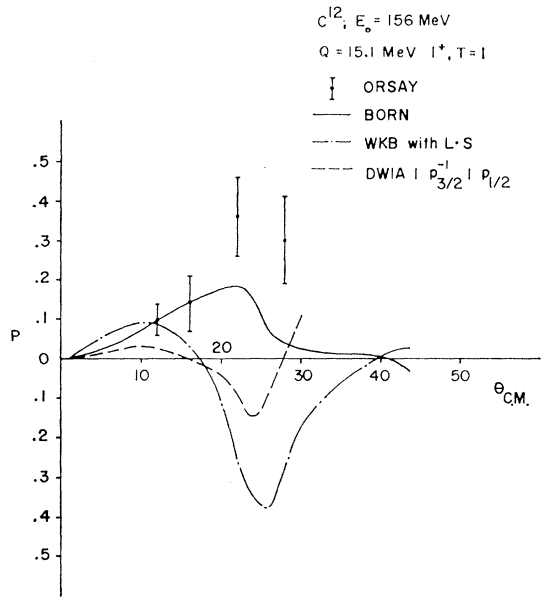

FIG. 8. Polarization for the 1^+ $T=1$ at 15.1 MeV of C^{12}. Data from Ref. 23. The effect of the spin-orbit term is in the wrong direction. Again the final-state configuration used in DWIA is pure $(1p_{3/2})^{-1}\,1p_{1/2}$.

3. $Q=12.7$ MeV: 1^+ $T=0$

Figure 6 compares the predicted cross section for the Gillet vector 1^+ $T=0$ at 14 MeV with experimental data. There is little agreement in shape and the cross section is predicted a factor of 10 too high. The experimental shape suggests an l forbidden transition. The simple j-j coupling model is quite useless for this magnetic transition. A calculation with intermediate coupling would be necessary for any valid comparison.

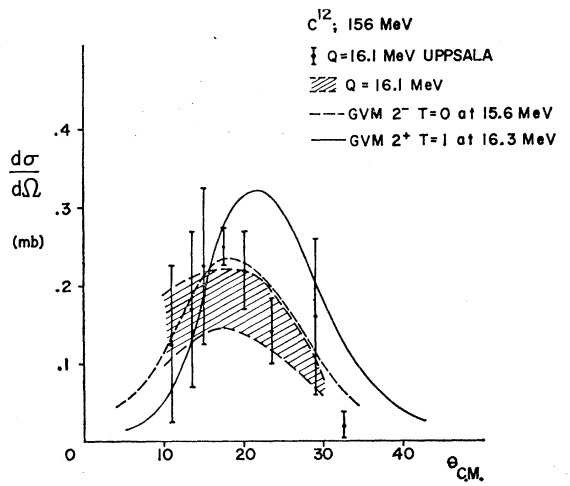

FIG. 9. Cross section of 16.1-MeV level of C^{12}. Bars are from Ref. 16 and shaded area from Ref. 23. From the cross section alone, 2^- $T=0$ state is favored. (See text.)

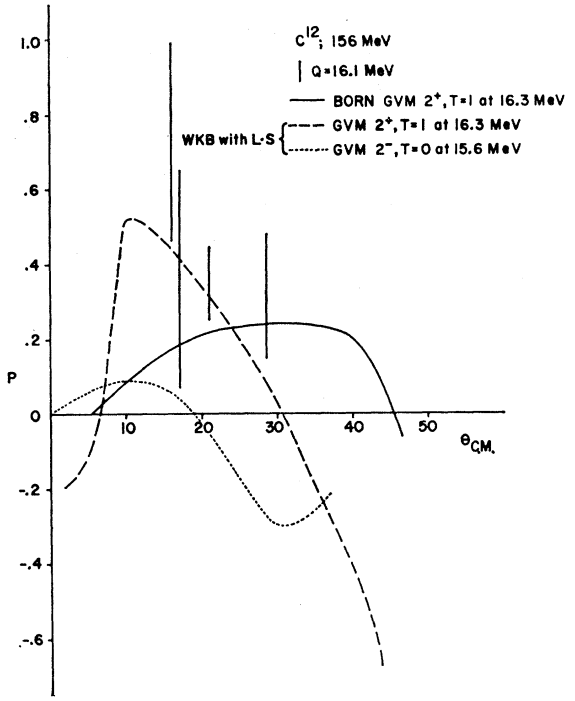

FIG. 10. Polarization due to 16.1-MeV level of C^{12}. Data from Ref. 23. Here polarization is consistent with 2^+ $T=1$ level. (See text.)

4. $Q=15.1$ MeV: 1^+ $T=1$

The form factor computed from the Gillet vector 1^+ $T=1$ at 16.6 MeV which corresponds to j-j coupling gives a cross section about 3 times larger than experiment (Fig. 7). This level has been extensively studied theoretically, using intermediate coupling, and also

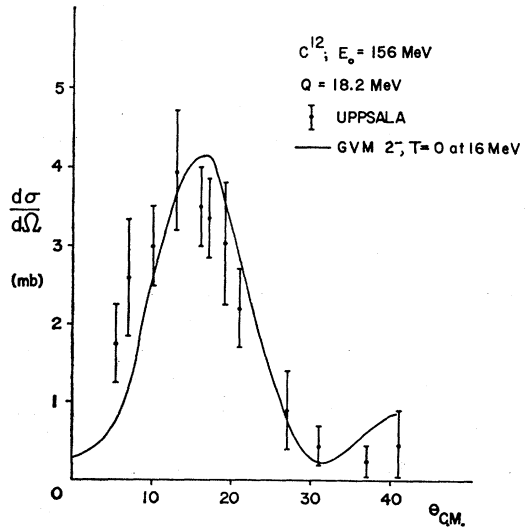

FIG. 11. Cross section of 18.2 MeV level of C^{12}. Gillet vector for 2^- $T=0$ level at 16 MeV gives good agreement with data from Ref. 16.

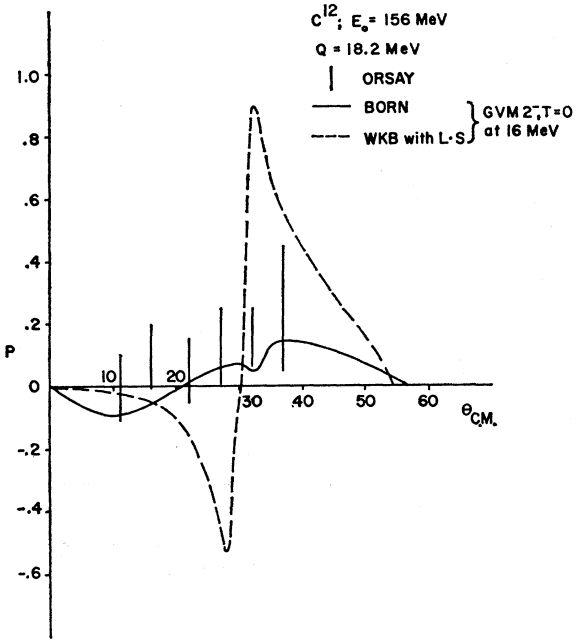

FIG. 12. Polarization due to 18.2-MeV level of C^{12}. Theoretical curves are computed from the Gillet vector 2^- $T=0$ level at 16 MeV. Data from Ref. 23.

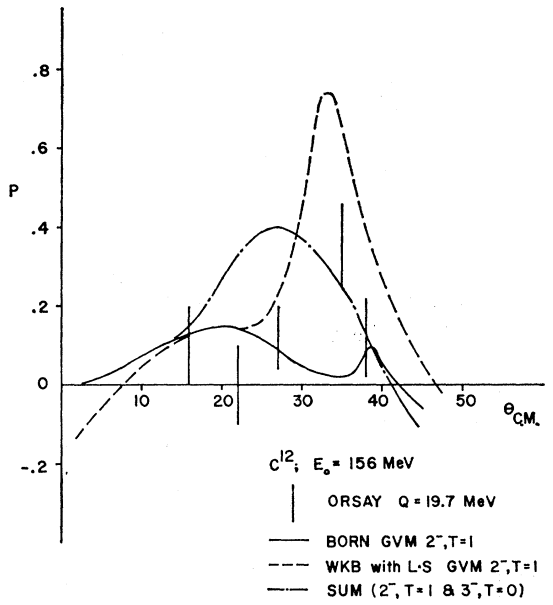

FIG. 14. Polarization of 19.3-MeV level of C^{12}. Data from Ref. 23. The curve labeled "sum" is the average of the polarization from 2^- $T=1$ at 19.3 MeV and 3^- $T=0$ at 19.5 MeV.

experimentally. Kurath,[21] on the basis of electron-scattering analysis, and Kawai *et al.*,[22] from the analysis of the β decay of B^{12} and N^{12}, conclude that the form factor agrees best with intermediate coupling with the parameter $\xi=6.0$ ($\xi=\infty$ for the j-j limit). The reduced $M1$ matrix which is the best compromise fit to the

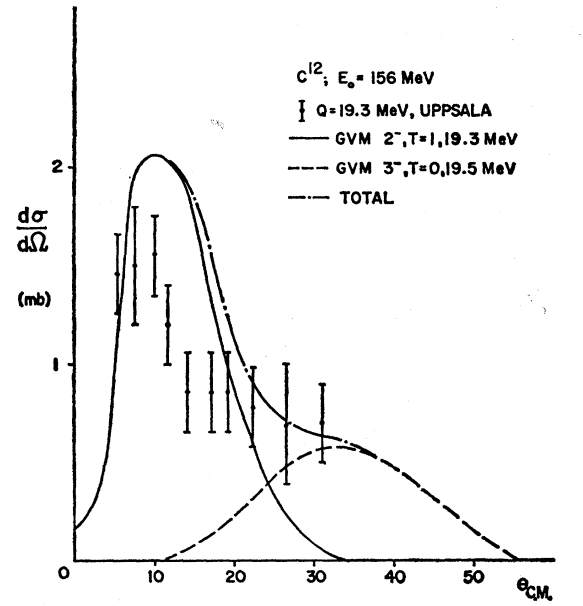

FIG. 13. Cross section of 19.3-MeV level of C^{12}. Data from Ref. 16. At small angles, a reduction of theoretical prediction by 30–40% would improve the agreement with data. (See text.)

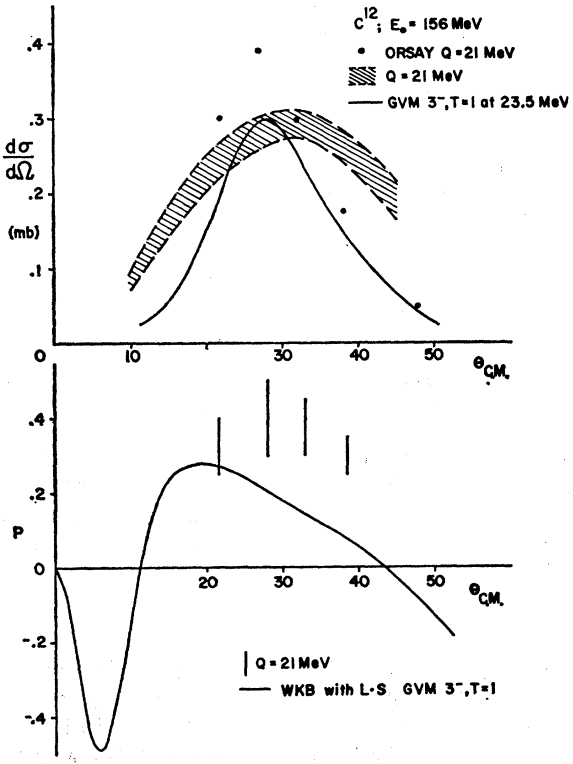

FIG. 15. Cross section and polarization of 21-MeV level of C^{12}. Points are from Ref. 20. The shaded area and bars for the polarizations are from Ref. 23. Predicted polarization is too small.

[21] D. Kurath, Phys. Rev. 134, B1025 (1964).
[22] M. Kawai, T. Teraswa, and K. Izumo, Progr. Theoret. Phys. (Kyoto) 27, 404 (1962).

electron-scattering and photon data is estimated to be $B_{M1}=1.13$ at zero momentum transfer (see Ref. 21). j-j coupling gives $B_{M1}=3.75$ in the same limit, so, as the radial parts of the form factor are the same, we have reduced the cross section calculated from the Gillet vector by a factor of 3.75/1.13 to give the equivalent of the electron-scattering-data best-fit form factor. The electron-scattering data did not determine the best value of the harmonic-oscillator constant too closely, so two values were used in the present work: $\alpha=0.2$ F^{-2} and $\alpha=0.37$ F^{-2}, the standard value for C^{12}. The discrimination from the proton-scattering data is about

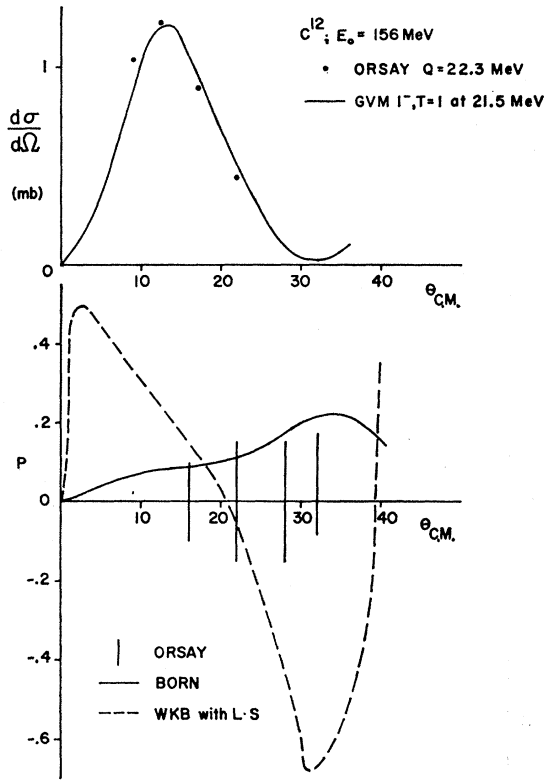

FIG. 16. Cross sections and polarization of the 1^- $T=1$ level of C^{12} at 22.3 MeV. Data for the cross section from Ref. 20 and polarization from Ref. 23.

comparable to that obtained from the electron-scattering data, which give, therefore, comparable information for this level. Polarization with and without optical spin are very different, and neither shows agreement with the experimental data[23] (Fig. 8).

5. $Q=16.1$ MeV

In Figs. 9 and 10 predictions from the Gillet vectors 2^- $T=0$ (15.6 MeV) and 2^+ $T=1$ (16.3 MeV) are compared with the experimental data for $Q=16.1$ MeV. The 2^- $T=0$ prediction is in good agreement with the

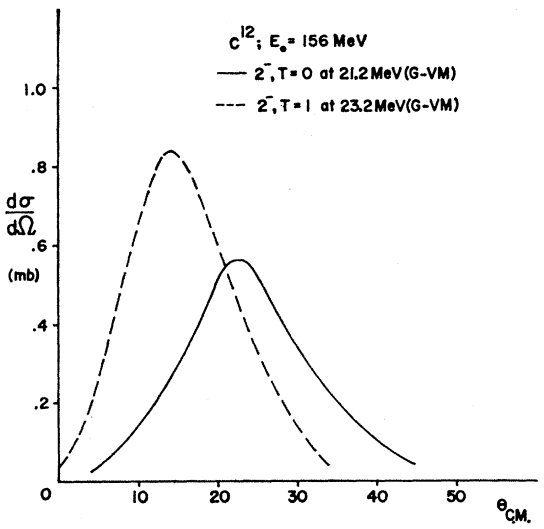

FIG. 17. Cross sections predicted for the Gillet vectors 2^- $T=0$ (21.2 MeV) and 2^- $T=1$ (23.2 MeV) of C^{12}.

cross-section data, and disagrees with the polarization data. The 2^+ $T=1$ level gives polarization consistent with the data, but gives poor agreement with the cross section. At 45-MeV incident proton energy, with much better resolution, the level seen at this Q value is the well-known 2^+ $T=1$ level at 16.1 MeV.[24] Segel *et al.*[25] demonstrate the existence of a 2^- level at 16.56 MeV, but give it as probably 2^- $T=1$. Better resolution is needed to decide whether the excitation observed in the high-energy proton scattering is due entirely to the 2^+

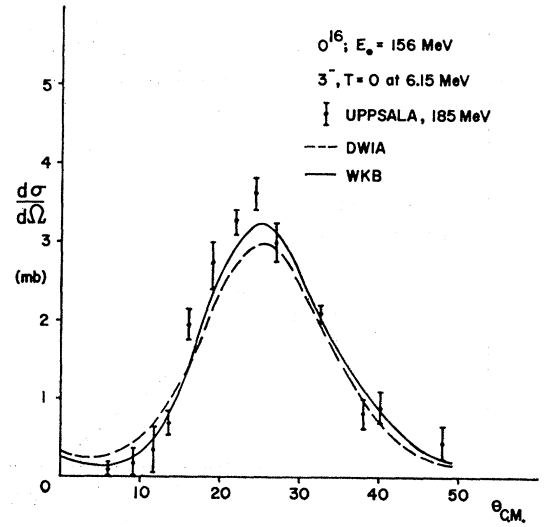

FIG. 18. Cross sections of the 3^- $T=0$ level at 6.15 MeV of O^{16}. Data from Ref. 16. 0^+ level at 6.05 MeV is not resolved in the data. DWIA and WKB agree with each other quite well.

[23] B. Tatischeff, thesis, 1966 (unpublished).

[24] I. Slaus (private communication).

[25] R. Segel, S. Hanna, and R. Allas, Phys. Rev. 139, B818 (1965).

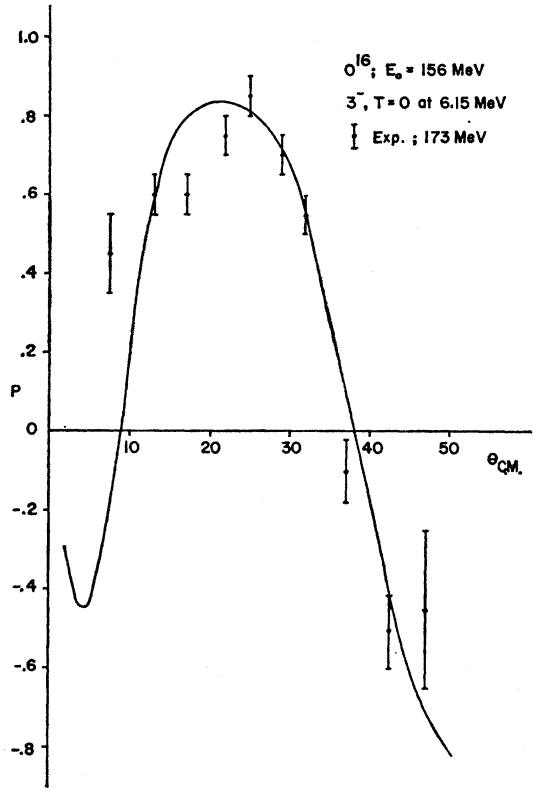

FIG. 19. Polarization due to the 3^- $T=0$ level at the 6.15 MeV level of O^{16}. Data from Ref. 19. DWIA calculation of Ref. 2, not shown here, predicts essentially the same polarization for this level as WKB.

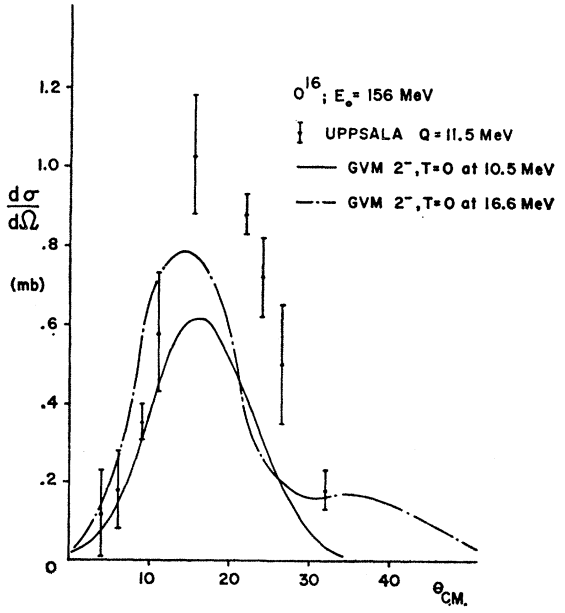

FIG. 20. Cross section of 2^- $T=0$ level. The form factors for 2^- $T=0$ at 10.5 MeV and at 16.6 MeV are compared. Data from Ref. 16.

$T=1$ level, or whether there is another unresolved 2^- excitation.

6. $Q=18.2$ MeV

Agreement between the predicted cross sections and the data is excellent as shown in Fig. 11, indicating that the form factor computed from the vector 2^- $T=0$ at 16 MeV is good. The polarization in the Born approximations shows spin-flip characteristics discussed in KMT (Fig. 12). The fluctuations near the diffraction minimum of the cross sections are in accordance with the predictions of Nishimura and Ruderman.[26] No such state is found in this excitation energy region in Ref. 25, which logs a 3^- probably $T=0$ state at 18.36 MeV, and a 0^- state at 18.40 MeV, so this may be new information.

7. $Q=19.3$ MeV

In Fig. 13, we show the predicted cross section from the vectors 2^- $T=1$ at 19.3 MeV and 3^- $T=0$ at 19.5

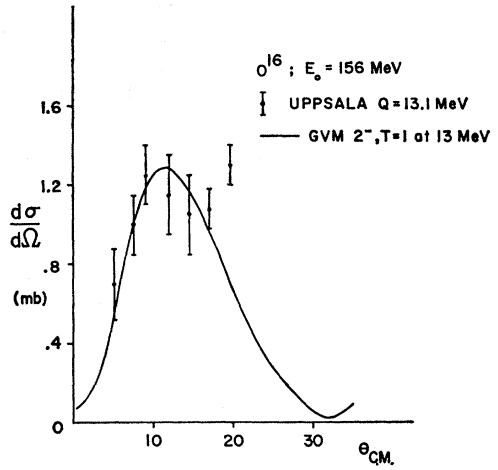

FIG. 21. Cross section of the level 2^- $T=1$ at 13.1 MeV. Agreement is good, indicating that the theoretical form factor used is reasonable.

MeV together with the data for this Q value. At forward angles where the 2^- contribution is dominant, a reduction of the theoretical prediction by 30–40% would be in better agreement with experiment. A level with this Q value is seen in electron scattering at backward angles.[27] The observed cross section agrees with that predicted for the 2^- $T=1$ level if the theoretical calculation is reduced by 50%.[28] Thus we have substantial agreement between electron and proton scattering as the form factors used in the two calculations are similar. This state is one of the giant magnetic quadrupole states largely responsible for muon capture. An analogous state appears at 20.2 MeV in O^{16}. In Fig. 14,

[26] K. Nishimura and R. Ruderman, Phys. Rev. **106**, 558 (1957).
[27] J. Goldemberg and W. C. Barber, Phys. Rev. **134**, B963 (1964).
[28] T. DeForest, Jr., Phys. Rev. **139**, B1217 (1965).

predicted polarizations and data are compared. It is difficult to draw any meaningful conclusions from the figure. The curve labeled "sum" is the average polarization for 2^- $T=1$ and 3^- $T=0$ states as calculated by

$$P=\left(\frac{d\sigma}{d\Omega}(2^-)P(2^-)+\frac{d\sigma}{d\Omega}(3^-)P(3^-)\right)\Big/\left(\frac{d\sigma}{d\Omega}(2^-)+\frac{d\sigma}{d\Omega}(3^-)\right).$$

8. Q=21 MeV

The form factor for the vector 3^- $T=1$ at 23.5 MeV gives a cross section in fair agreement with the data (Fig. 15). The predicted polarization is too small.

9. Q=22.3 MeV

The observed cross section for this level is in agreement with that predicted for the 1^- $T=1$ vector at 21.5 MeV as shown in Fig. 16. The predicted polarization shows large fluctuations, not observed experimentally, but this state is undoubtedly part of the giant dipole resonance as noticed previously by Sanderson.

Differential cross sections for the vector 2^- $T=0$ at 21.2 MeV and 2^- $T=1$ at 23.2 MeV are given in Fig. 17. No data are available for comparison.

B. O^{16}

1. Q=6.15 MeV: 3^- T=0

The observed cross section is larger than the theoretical predictions of both WKB and DWIA by about 10% (Fig. 18). The experiment did not resolve the 0^+ $T=0$ level at 6.05 MeV. Electron scattering from this level has been observed and is about 25% higher at peak than the predictions of the Gillet vector. If the cross section of the 0^+ is taken to be the same as the observed cross section of the lowest 0^+ level in C^{12}, this removes most of the discrepancy, so again there is agreement with experiment and complete agreement between proton and electron inelastic scattering. The predicted polarization is compared with data in Fig. 19.

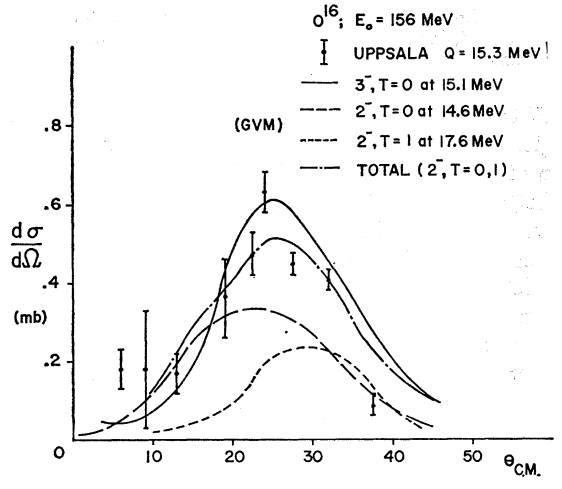

FIG. 22. Cross section of the 15.3 MeV level of O^{16}. The Gillet vector 3^- $T=0$ at 15.1 MeV gives reasonably good agreement as does the sum of the vectors 2^- $T=0$ at 14.6 MeV and 2^- $T=1$ at 17.6 MeV. Data from Ref. 16.

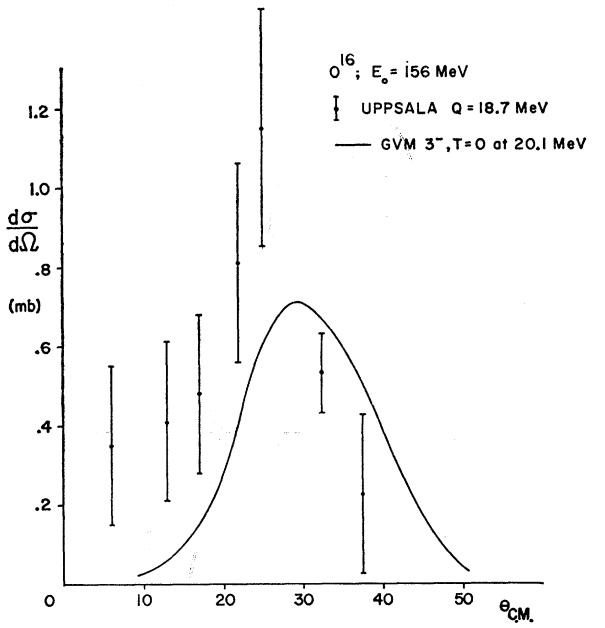

FIG. 23. Cross section of the 18.7-MeV level of O^{16}. Large experimental values (Ref. 16) at small angles suggest the presence of states of lower multipolarity.

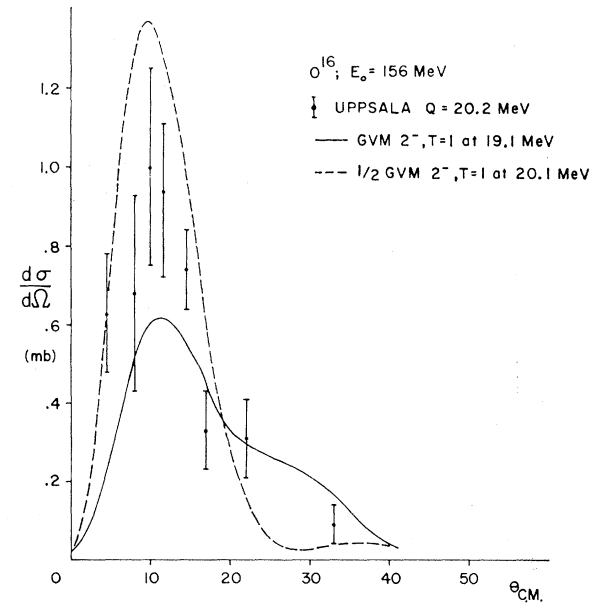

FIG. 24. Cross section of the 20.2-MeV level of O^{16}. The solid line is too low. The dashed curve is in reasonable agreement with experiment.

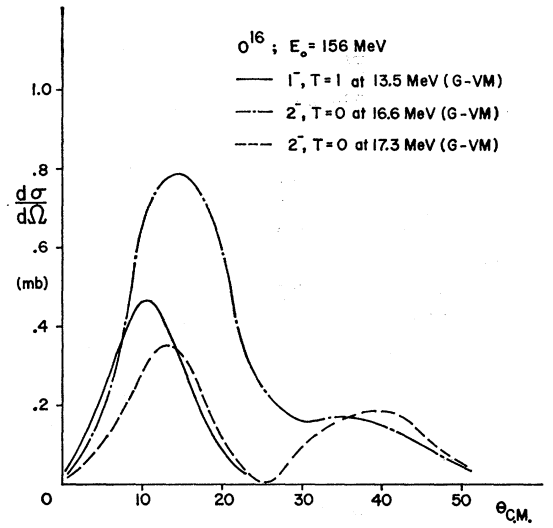

FIG. 25. Cross sections predicted for the Gillet vectors 1^- $T=1$ (13.5 MeV), 2^- $T=0$ (16.6 MeV), and 2^- $T=0$ (17.3 MeV).

Since there are no data points at forward angles, we can only note the general agreement with experiment.

2. $Q=11.5$ MeV

The experimental result for this level is compared with the Gillet vectors 2^- $T=0$ at 10.5 MeV and 16.6 MeV in Fig. 20. The latter is in better agreement with experiment. It is essentially similar to the vector previously calculated by Erickson,[7,16] which gives good agreement with experiment.

3. $Q=13.1$ MeV

The form factor for the vector 2^- $T=1$ at 13.0 MeV gives excellent agreement with the data, again being essentially the same as that previously calculated by Erickson[7,16] (Fig. 21).

4. $Q=15.3$ MeV

The theoretical vector 3^- $T=0$ at 15.1 MeV gives fair agreement with experiment, as pointed out by Haybron (Fig. 22). However, equally good agreement is obtained with the sum of the cross sections for the theoretical vectors 2^- $T=0$ at 14.6 MeV and 2^- $T=1$ at 17.6 MeV.

5. $Q=18.7$ MeV

The prediction of the vector 3^- $T=0$ at 20.1 MeV is compared in Fig. 23 with the observed cross section at $Q=18.7$ MeV. Large values of the cross section at forward angles suggest unresolved lower multipoles.

6. $Q=20.2$ MeV

A level with this Q value is seen in electron scattering at backward angles.[29] The observed cross section agrees with the prediction for a 2^- $T=1$ level, except that the theoretical prediction is too high by a factor of 2 (Ref. 28). In the present case the cross section is compared in Fig. 24 with the theoretical predictions for the vector 2^- $T=1$ at 19.1 MeV and also with half the theoretical cross section for the vector 2^- $T=1$ at 20.1 MeV. Reasonable agreement is obtained for the latter case. Since the form factors of the Gillet vector at 20.1 MeV and the DeForest vector used in the electron-scattering analysis of Ref. 28 are similar for this level, we again have good agreement between proton and electron scattering.

In Fig. 25, predictions of the cross sections for the levels 1^- $T=1$ at 13.5 MeV, 2^- $T=0$ at 16.6 MeV, and 2^- $T=0$ at 17.3 MeV are shown. No data are available to us for comparison.

V. CONCLUSION

By way of detailed comparison, we have shown that the WKB predictions of cross sections and polarizations for the inelastically scattered protons at an incident energy of 156 MeV are in close agreement with the DWIA calculations. Unfortunately, both WKB and DWIA fail to predict the polarizations correctly, especially for the spin-flip final states. One of the reasons for this failure may be that the shape of the spin-orbit optical potential was not fitted to the elastic-polarization data.

There is surprisingly detailed agreement between experiment and the predictions of a particle-hole model, despite the simple assumptions of j-j coupling and random-phase approximation. A notable exception to this is the 1^+ level of C^{12}, where the deficiencies of the j-j coupling model are apparent, as is well known.

We have found a striking correlation between proton and electron inelastic scattering. For the states considered here, the two methods yield identical information about nuclear structure. This may be taken as providing an over-all check on the validity of the impulse approximation used in the proton-scattering analysis.

ACKNOWLEDGMENT

The authors wish to thank F. Petrovich for checking some of the form-factor calculations.

APPENDIX

The radial wave functions used in evaluating the form factors are:

$$R_{1,l}=\pi^{-1/4}\alpha^{3/4}\left(\frac{2^{l+2}}{(2l+1)!!}\right)^{1/2}\alpha^{l/2}r^l e^{-\alpha r^2/2},$$

$$R_{2,l}=\pi^{-1/4}\alpha^{3/4}\left(\frac{2^{l+3}}{(2l+3)!!}\right)^{1/2}\alpha^{l/2}r^l\left[\frac{2l+3}{2}-\alpha r^2\right]e^{-\alpha r^2/2}.$$

[29] G. J. Vanpraet and W. C. Barber, Nucl. Phys. **79**, 550 (1966).

C^{12}

$\langle 1^- \rangle$

$$F^{101} = -0.225\alpha^2 e^{-\alpha r^2}(C_1 r + C_2 \alpha r^3),$$
$$F^{111} = 0.225\alpha^2 e^{-\alpha r^2}(D_1 r + D_2 \alpha r^3).$$

$T=1$:

E (MeV)	C_1	C_2	D_1	D_2
17.7	4.59	−2.7	3.24	−2.17
21.5	0.674	−2.77	0.682	1.34

$\langle 1^+ \rangle$

$$F^{011} = 0.225\alpha^{3/2} e^{-\alpha r^2}(C_1 + C_2 \alpha r^2 + C_3 \alpha^2 r^4),$$
$$F^{211} = 0.225\alpha^{5/2} e^{-\alpha r^2}(D_1 r^2 + D_2 \alpha r^4).$$

$T=0$:

E (MeV)	C_1	C_2	C_3	D_1	D_2
14.0	−0.485	2.34	0.53	−1.54	0.167

$T=1$:

16.6	−0.137	2.600	0.336	−1.064	0.043

$\langle 2^- \rangle$

$$F^{112} = 0.225\alpha^2 e^{-\alpha r^2}(C_1 r + C_2 \alpha r^3),$$
$$F^{312} = 0.225\alpha^3 e^{-\alpha r^2} D_1 r^3.$$

$T=0$:

E (MeV)	C_1	C_2	D_1
15.6	2.46	0	0.78
16.0	−5.04	4.09	0.398
21.2	−0.148	1.57	−0.97

$T=1$:

18.2	−5.0	2.36	−0.256
19.3	−0.249	3.29	0.645
23.2	−0.312	1.51	−1.045

$\langle 2^+ \rangle$

$$F^{202} = 0.225\alpha^{5/2} e^{-\alpha r^2}(C_1 r^2 + C_2 \alpha r^4),$$
$$F^{212} = 0.225\alpha^{5/2} e^{-\alpha r^2}(D_1 r^2 + D_2 \alpha r^4).$$

$T=0$:

E (MeV)	C_1	C_2	D_1	D_2
4.8	5.52	−0.183	−3.536	0.665

$T=1$:

16.3	1.980	−0.027	−2.64	−0.083

$\langle 3^- \rangle$

$$F^{303} = C_1 \alpha^3 r^3 e^{-\alpha r^2},$$
$$F^{313} = D_1 \alpha^3 r^3 e^{-\alpha r^2}.$$

$T=0$:

E (MeV)	C_1	D_1
12.8	−0.545	0.178
19.5	0.2	−0.443

$T=1$:

18.4	−0.306	−0.0945
23.5	0.39	−0.443

O^{16}

$\langle 1^- \rangle$

$$F^{101} = -0.225\alpha^2 e^{-\alpha r^2}(C_1 r + C_2 \alpha r^3),$$
$$F^{111} = 0.225\alpha^2 e^{-\alpha r^2}(D_1 r + D_2 \alpha r^3).$$

$T=1$:

E (MeV)	C_1	C_2	D_1	D_2
13.5	−3.32	1.93	4.56	−2.85

$\langle 2^- \rangle$

$$F^{112} = 0.225\alpha^2 e^{-\alpha r^2}(C_1 r + C_1 \alpha r^3),$$
$$F^{312} = 0.225\alpha^3 e^{-\alpha r^2} D_1 r^3.$$

$T=0$:

E (MeV)	C_1	C_2	D_1
10.5	0.0056	1.72	−0.369
14.6	0.0056	−0.949	1.78
16.6	−0.068	2.225	1.74
17.3	−0.564	3.72	−0.0219

$T=1$:

13.0	0.34	1.56	−0.475
17.6	−0.119	−0.15	1.96
19.1	2.88	0.08	1.04
20.1	−4.84	4.38	0.62

$\langle 3^- \rangle$

$$F^{303} = -0.380\alpha^3 r^3 e^{-\alpha r^2} C_1,$$
$$F^{313} = +0.380\alpha^3 r^3 e^{-\alpha r^2} D_1.$$

$T=0$:

E (MeV)	C_1	D_1
6.25	−1.93	0.839
15.1	0.809	0.519
20.1	−0.621	−1.268

$T=1$:

E (MeV)	C_1	D_1
12.7	−0.854	1.14
18.5	0.822	−0.226
24.1	−1.06	−1.14